Title

Rapidly changing high-latitude seasonality: implications for the 21st century carbon cycle in Alaska

Journal

Environmental Research Letters, 17(1)

ISSN

1748-9318

Authors

Shirley, Ian A
Mekonnen, Zelalem A
Grant, Robert F
et al.

Publication Date

2022

DOI

10.1088/1748-9326/ac4362

Peer reviewed

ENVIRONMENTAL RESEARCH
LETTERS

LETTER • OPEN ACCESS

Rapidly changing high-latitude seasonality: implications for the 21st century carbon cycle in Alaska

IOP Publishing Environ. Res. Lett. 17 (2022) 014032 https://doi.org/10.1088/1748-9326/ac4362

ENVIRONMENTAL RESEARCH
LETTERS

OPEN ACCESS

RECEIVED
15 July 2021

REVISED
10 December 2021

ACCEPTED FOR PUBLICATION
15 December 2021

PUBLISHED
5 January 2022

LETTER

Rapidly changing high-latitude seasonality: implications for the 21st century carbon cycle in Alaska

Ian A Shirley[1,2,*], Zelalem A Mekonnen[1], Robert F Grant[3], Baptiste Dafflon[1], Susan S Hubbard[1] and William J Riley[1]

[1] Climate and Ecosystem Sciences Division, Lawrence Berkeley National Laboratory, Berkeley, CA, United States of America
[2] Department of Physics, University of California-Berkeley, Berkeley 94720-3114, CA, United States of America
[3] Department of Renewable Resources, University of Alberta, Edmonton, Canada
[*] Author to whom any correspondence should be addressed.

E-mail: IShirley@lbl.gov

Keywords: seasonality, high-latitudes, carbon cycle, climate change

Supplementary material for this article is available online

Abstract

Seasonal variations in high-latitude terrestrial carbon (C) fluxes are predominantly driven by air temperature and radiation. At present, high-latitude net C uptake is largest during the summer. Recent observations and modeling studies have demonstrated that ongoing and projected climate change will increase plant productivity, microbial respiration, and growing season lengths at high-latitudes, but impacts on high-latitude C cycle seasonality (and potential feedbacks to the climate system) remain uncertain. Here we use *ecosys*, a well-tested and process-rich mechanistic ecosystem model that we evaluate further in this study, to explore how climate warming under an RCP8.5 scenario will shift C cycle seasonality in Alaska throughout the 21st century. The model successfully reproduced recently reported large high-latitude C losses during the fall and winter and yet still predicts a high-latitude C sink, pointing to a resolution of the current conflict between process-model and observation-based estimates of high-latitude C balance. We find that warming will result in surprisingly large changes in net ecosystem exchange (NEE; defined as negative for uptake) seasonality, with spring net C uptake overtaking summer net C uptake by year 2100. This shift is driven by a factor of 3 relaxation of spring temperature limitation to plant productivity that results in earlier C uptake and a corresponding increase in magnitude of spring NEE from −19 to −144 gC m^{-2} $season^{-1}$ by the end of the century. Although a similar relaxation of temperature limitation will occur in the fall, radiation limitation during those months will limit increases in C fixation. Additionally, warmer soil temperatures and increased carbon inputs from plants lead to combined fall and winter C losses (163 gC m^{-2}) that are larger than summer net uptake (123 gC m^{-2} $season^{-1}$) by year 2100. However, this increase in microbial activity leads to more rapid N cycling and increased plant N uptake during the fall and winter months that supports large increases in spring NPP. Due to the large increases in spring net C uptake, the high-latitude atmospheric C sink is projected to sustain throughout this century. Our analysis disentangles the effects of key environmental drivers of high-latitude seasonal C balances as climate changes over the 21st century.

1. Introduction

Surface air temperature and solar radiation exhibit strong seasonality and shape seasonal and annual cycles of plant and microbial activities in high-latitude ecosystems (Ernakovich *et al* 2014). Late snowmelt, cool summers, and short autumn days lead to short and relatively unproductive growing seasons (Billings 1973, Ernakovich *et al* 2014), and frozen soils and harsh winters inhibit organic matter decomposition (Mikan *et al* 2002). The high latitudes are particularly susceptible to anthropogenic climate warming (Serreze *et al* 2009), and recent rapid increases in air temperature are projected to

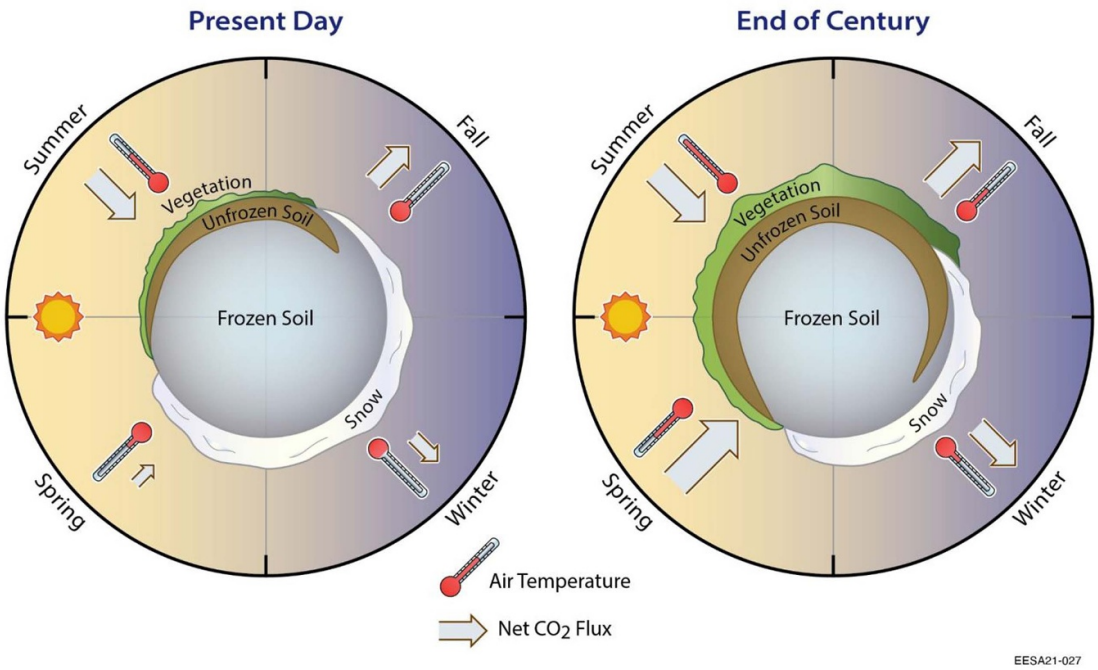

Figure 1. 21st century climate warming will shift the seasonality of the C cycle across Alaska. As depicted in this schematic, there will be important changes to the seasonality of high-latitude NEE throughout the 21st century. Relaxation of temperature limitation to plant productivity will cause large increases in spring net C uptake. Warming air and soil temperatures, coincident with persistent radiation limitation to plant productivity, will cause large increases in fall and winter net C losses. Summer net C uptake also increases with increasing air temperatures and CO_2 concentrations, but will be smaller in magnitude than spring C uptake and combined fall and winter C losses by year 2100. Also depicted are changes to snow, soil freeze and thaw, and vegetation dynamics that result from and contribute to changing C cycle seasonality. Changes to soil biogeochemical processes during fall and winter, including N mineralization and uptake, are implied in the changes to soil freeze and thaw state. The seasons are equinox based (i.e. spring is the period 21 March–20 June, summer is the period 21 June–20 September, fall is the period 21 September–20 December, and winter is the period 21 December–20 March).

accelerate throughout the 21st century (Serreze and Barry 2011, Box *et al* 2019). This climate warming will shift the relative effects of temperature and radiation limitations on biological activity, and therefore the C cycle (figure 1). While previous modeling and observation-based studies have demonstrated that climate warming will induce increased C fixation and a longer growing season at high-latitudes (Arora and Boer 2014, Ito *et al* 2016, Gallego-Sala *et al* 2018, Tharammal *et al* 2019), the impacts of climate change on the seasonality of high-latitude C cycling remain uncertain.

The amplitude of the seasonal cycle of atmospheric CO_2 concentrations in northern latitudes has been increasing steadily over the past 50 years and has been explained by changes in the seasonality of the terrestrial C cycle (Graven *et al* 2013). Earlier leaf-out in the spring (Commane *et al* 2017, Xu *et al* 2018, Winkler *et al* 2019) and higher productivity and allocation to woody biomass during the summer (Leffler *et al* 2016, Mekonnen *et al* 2018) increase the regional C sink strength. Fall and winter soil warming increases regional C losses due to higher soil microbial respiration rates (Commane *et al* 2017, Parazoo *et al* 2018, Natali *et al* 2019). The sum of these seasonal changes, which represents the balance between climate induced changes in vegetation productivity and microbial activity, has important implications for the global C cycle as the large organic C stocks stored in permafrost soils (Schuur *et al* 2015) have the potential to drive important climate feedbacks (Gallego-Sala *et al* 2018, Rogelj *et al* 2019).

Model predictions of current high-latitude ecosystems mostly suggest that they are net C sinks (McGuire *et al* 2012, Arora and Boer 2014, Ito *et al* 2016), while several recent observation-based studies indicate the opposite. For example, Natali *et al* (2019), using machine learning to spatially and temporally extrapolate high-latitude measurements, predicted higher fall and winter regional C losses than did a suite of process-models for the years 2003–2017. The non-growing season losses predicted by Natali *et al* (2019) are also larger than the growing season uptake predicted by the process-models. Commane *et al* (2017), using aircraft observations and upscaled eddy covariance measurements, argued that high rates of fall respiration caused Alaska to be a C source between 2012 and 2014. These discrepancies between process-model predictions and observation-based estimates raise concerns that missing or misrepresented cold-season mechanisms could bias process-model predictions of high-latitude ecosystem responses to climate change. Consideration of seasonal changes in C fluxes is needed to disentangle mismatches between

modeling and observation-based studies, to provide insight into driving forces behind model results, and to identify important measurements needed to evaluate and build confidence in model predictions.

Here, we examine climate change impacts on Alaska C cycle seasonality using a well-tested mechanistic ecosystem model, *ecosys*. This study is also motivated by the large reported differences in models and observation-based assessments of C cycle seasonality dynamics, particularly during the fall and winter (Commane *et al* 2017, Xu *et al* 2018, Natali *et al* 2019, Winkler *et al* 2019). Because of its rich process representations (e.g. process-specific temperature cutoffs and activation energies that can represent low-temperature biogeochemical activity and climate-change acclimation, mineralization and plant nutrient uptake that is driven by availability and capability rather than photosynthetic activity), *ecosys* is well-suited to address these questions. After further evaluating the model and showing it is broadly consistent with recent site- and regional-scale observations (including those mentioned above), we apply it to analyze processes that control seasonality of plant and microbial activity, and explore how these controls are expected to change over the 21st century and how these changes will affect regional ecosystem C budgets.

2. Data and methods

2.1. Model description

Ecosys is an hourly time-step ecosystem model with multiple canopy, snow, and soil layers. The tightly coupled C, energy, nutrient, and water cycles operate across a wide range of temporal, and spatial scales. Key model processes are outlined below, and a comprehensive description is given in the supplementary material of Mekonnen *et al* (2019).

Each grid cell is forced with meteorological inputs and the model is initialized with prescribed seed densities for five plant functional types (PFTs) (deciduous, evergreen, sedge, moss, lichen). PFT-specific functional traits (i.e. CO_2 fixation kinetics, leaf optical properties, phenology, morphology, and root traits) result in emergent PFT variation in phenology, irradiance, CO_2 fixation rate, and water uptake. Functional traits differ for PFTs seeded in the boreal forest compared with those seeded in the tundra (figure 2). The model represents a multi-layer canopy, a residue layer, and multi-layer soil column. Leaf properties (including azimuth and angle), solar incidence angle, and light availability dictate propagation and absorption of direct and diffuse shortwave radiation in the canopy (Grant and Baldocchi 1992). Canopy energy balance, calculated using first-order closure schemes and by setting the sum of heat fluxes to zero, is tightly coupled to the water cycle through evapotranspiration. Heat and water transfers between the atmosphere, canopy, and soil column determine the temperature, water content, and ice content of each soil layer.

Coupling between carboxylation and CO_2 diffusion determines canopy CO_2 fixation (Grant *et al* 2001). The Farquhar biogeochemical growth model (Farquhar *et al* 1980) is used to calculate carboxylation as the lesser of the light-limited and CO_2 limited carboxylation rates. Stomatal conductance balances water availability and maintenance of a fixed internal-to-ambient CO_2 ratio (Grant and Flanagan 2007). In the light limited carboxylation rate, potential electron transport rate is a hyperbolic function of radiation. Leaf temperature directly controls fixation rates through a modified Arrhenius temperature dependence of maximum rate constants, Michaelis–Menten coefficients, light-saturated electron transport rates, and an exponential temperature dependence of CO_2 and O_2 aqueous solubility. The modified Arrhenius temperature dependencies include low and high deactivation temperatures and a constant offset to account for thermal adaptation of each PFT. Air temperatures indirectly impact CO_2 fixation by modifying nutrient mineralization and uptake rates, boundary layer resistances, and evapotranspiration rates.

Photosynthesized sugars are allocated to non-structural C pools and oxidized to support first maintenance respiration and then shoot and root growth and active nutrient uptake. Oxidation rates and maintenance respiration requirements depend on a modified Arrhenius function of temperature that includes low and high temperature cutoffs and a thermal acclimation offset.

For winter deciduous PFTs, temperature-driven leaf onset (leaf offset) occurs after accumulated hours above (below) a set canopy temperature cross a set threshold. For evergreen PFTs, leaf dehardening (hardening) occurs after accumulated hours in increasing (decreasing) photoperiods crosses a set threshold. Leaf and root senescence for all PFTs occurs when non-structural C oxidation cannot meet maintenance respiration demands.

Pools of soil organic matter (woody litter, non-woody litter, particulate organic matter, humus, microbial biomass) are partitioned into subsets of varying susceptibility to hydrolysis (Grant 2001). Decomposition of these pools produces dissolved organic C, which drives microbial growth when oxidized. Substrate availability, soil temperature (according to an Arrhenius functional form with a constant offset and low and high temperatures of deactivation), and soil water content control oxidation rates. Oxygen and nutrient availability may impose additional constraints. Plant nitrogen (N) and phosphorus (P) uptake rates are affected by nutrient mineralization and immobilization rates driven by microbial biomass C:N:P ratios (Grant 2014).

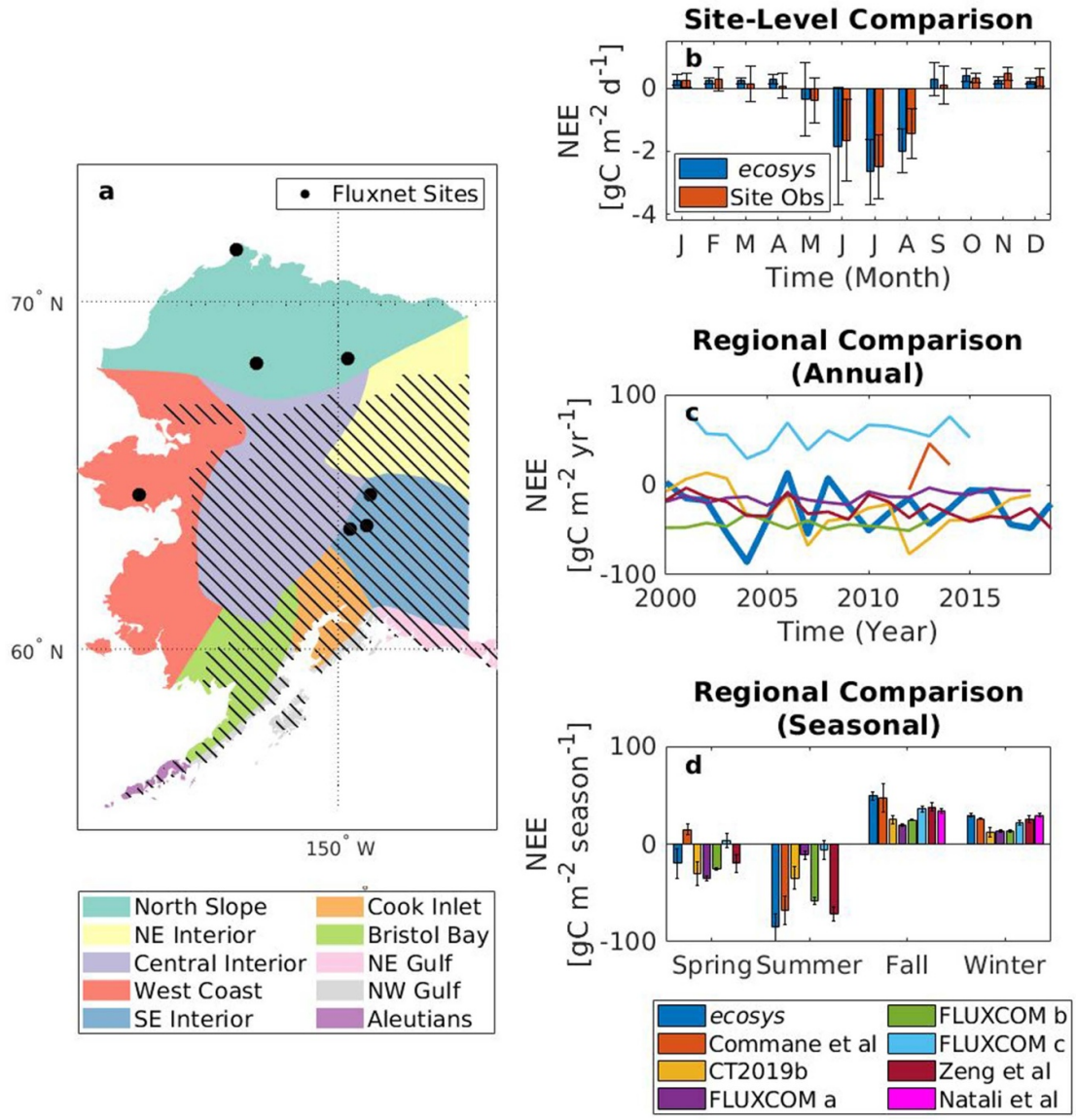

Figure 2. *Ecosys* accurately represents NEE at site and regional scales. (a) Map of the study region with climate zones, land cover types, and FLUXNET site locations. NOAA climate zones for Alaska are delineated by filled colors. The hatched regions are seeded with boreal forest PFTs and the unhatched regions are seeded with tundra PFTs. FLUXNET site locations are marked with black filled circles. (b) Comparison of FLUXNET measurements of NEE with *ecosys* outputs at 8 sites across Alaska. The simulations used for the FLUXNET comparison were forced with site weather data. Error bars denote the standard deviation observed and modelled across the sites. (c), (d) Seven observation-based estimates of Alaska NEE ((Commane *et al* 2017); CT2019b (Jacobson *et al* 2020); FLUXCOM (a)–(c) (forced with ERA5, CRUNCEP v6, and no weather forcing, respectively; Jung *et al* 2020); (Zeng *et al* 2020); (Natali *et al* 2019)) are compared with *ecosy* predictions for Alaska annual (c) and seasonal (d) NEE. Error bars represent the standard deviation across years of observation. The seasons are equinox based.

2.2. Model forcing and simulation design

The model was run at a 0.25° × 0.25° grid that covers Alaska. Clay and sand fraction, pH, cation exchange capacity, and bulk density were extracted from the Unified North America Soil Map (Liu *et al* 2013) and values for initial soil organic C content were extracted from the Northern Circumpolar Soil Carbon Database (Hugelius *et al* 2013). Surface air temperature, precipitation, incoming shortwave radiation, relative humidity and wind speed were taken from the North American Regional Reanalysis (NARR; Wei *et al* 2014) for the years 1979–2019. The first decade of the NARR record was used to spin-up the model over the years 1800–1978. NARR weather forcing for 2020–2100 was modified using seasonal anomalies from a CCSM4 ensemble member under the Representative Concentration Pathway 8.5 (RCP8.5). Since global carbon emissions are increasing at a rate consistent with RCP8.5, use of this high emissions scenario is common practice (Lee *et al* 2014, Lawrence *et al* 2015, Wieder *et al* 2015, McGuire *et al* 2018, Parazoo *et al* 2018). Historic CO_2 concentrations were used for 1800–2019, and CO_2 concentrations from RCP8.5 were used for 2020–2100. These simulations include N deposition taken from global spatially-distributed estimates (Dentener 2006, Wei *et al* 2014) and

stand-replacing fire events, with frequency derived from the Mean Fire Return Interval (MFRI) dataset of the LANDFIRE product (Rollins 2009).

2.3. Model evaluation

Ecosys representation of ecosystem C, nutrients, energy, and hydrological dynamics has been tested in many high-latitude sites. For example, modeled active layer depth matched long-term measurements at 28 Circumpolar Active Layer Monitoring sites (R^2 = 0.63; RMSE = 10 cm; Mekonnen *et al* 2021), modeled North American tundra gross primary production (GPP) matched upscaled EC tower measurements (geographically weighted regression, R^2 = 0.78; Mekonnen *et al* 2018), modeled tree composition of the Alaskan boreal forest agreed well with LANDFIRE–FCCS maps (Mekonnen *et al* 2019), and modeled NEE agreed well with EC tower measurements at 12 North American tundra and boreal sites ($0.6 < R^2 < 0.9$; Grant *et al* 2009, 2011, 2015, 2017). Additionally, *ecosys* accurately captured thermal and biological dynamics of short-term soil warming experiments at 4 sites across Alaska (Bouskill *et al* 2020). Fifteen studies of *ecosys* performance in high-latitude systems are described in the supplementary material (available online at stacks.iop.org/ERL/17/014032/mmedia).

Here we perform further validation of the *ecosys* model. Simulated soil temperatures at 24 locations were compared to data from the Soil Climate Analysis Network (SCAN; table S1; Schaefer *et al* 2007) and the Snow Telemetry (SNOTEL) Network (USDA Natural Resources Conservation Service 2020). Simulated NEE at 8 sites in Alaska was compared to data from Ameriflux EC towers (table S2). Where available, weather observations, rather than NARR forcings, were used to force the model for each Ameriflux site.

At the regional scale, we compared *ecosys* outputs with 7 observation-based estimates of monthly NEE across Alaska: (1) an estimate of NEE by Commane *et al* (2017) based on observed atmospheric CO_2 concentrations, remotely sensed data, and meteorological inputs; (2) NOAA's CarbonTracker (CT2019) estimates of NEE based on global measurements of atmospheric CO_2 concentration and an atmospheric transport model (Jacobson *et al* 2020); (3)–(5) three FLUXCOM estimates of NEE (FLUXCOM-RS-METEO-ERA5, FLUXCOM-RS-METEO-CRUNCEP, FLUXCOM-RS) based on machine-learning upscaling of global EC tower measurements using ERA5 weather forcing, CRUNCEP weather forcing, and no weather forcing, respectively (Jung *et al* 2020); (6) an estimate of winter CO_2 flux by Natali *et al* (2019) based on machine learning upscaling of site chamber, soda lime, and EC measurements; and (7) an alternate machine-learning upscaling of global EC tower measurements using ERA5 weather forcing produced by Zeng *et al* (2020).

2.4. Calculation of temperature and radiation limitation to net primary production (NPP)

Temperature and radiation limitations to plant productivity were quantified according to the methodology outlined in Donohue *et al* (2013), Keenan and Riley (2018), and Ukkola *et al* (2016). All daily modeled NPP values for the years 2010–2019 and 2090–2099 were combined and grouped by air temperature (incoming shortwave radiation) into bins of 1 °C (0.3 kWh m^{-2} d^{-1}). For each bin the 99th percentile NPP was calculated. Using breakpoint regression analysis, air temperatures and radiation levels that limit NPP, and the lowest air temperatures and radiation levels that do not limit NPP, were calculated. Temperature and radiation scalars were linearly interpolated between these values.

3. Results and discussion

3.1. Model evaluation and present day C cycle seasonality

In addition to the extensive validation of model performance in high-latitude ecosystems discussed above and listed in table S4, we also compared simulations of soil temperatures and NEE to site observations and regional observation-based estimates. At the site scale, *ecosys* soil temperatures at 5 cm depth agreed very well with measurements at 8 Soil Climate Analysis Network (SCAN) and 15 Snow Telemetry (SNOTEL) Network locations that are broadly representative of Alaskan climatic zones and land cover types (mean $R^2 = 0.70 \pm 0.11$, mean bias $= 0.09 \pm 1.46$ °C, and RMSE $= 4.22 \pm 1.41$ °C; figure S4, table S1). We also found excellent agreement with *ecosys* monthly NEE and EC tower measurements at eight Alaskan Ameriflux sites (mean $R^2 = 0.67 \pm 0.11$, mean bias $= -0.09 \pm 0.19$ gC m^{-2} d^{-1}, and Nash-Sutcliffe coefficient $= 0.41 \pm 0.56$ gC m^{-2} d^1; figure 2, table S2).

At the regional scale, we evaluated *ecosys* NEE against seven observation-based products (Commane *et al* 2017, Natali *et al* 2019, Jacobson *et al* 2020, Jung *et al* 2020, Zeng *et al* 2020). These products were generated by others, either through machine learning upscaling of site measurements or through estimation of land surface flux contributions to measured atmospheric CO_2 gradients using atmospheric transport models. We modeled an annual average NEE of -28 ± 25 gC m^{-2} yr^{-1} across Alaska for the years 2000–2019 (i.e. a net CO_2 sink from the atmosphere; uncertainty is expressed as standard deviation across years). The long-term mean modeled NEE is in excellent agreement with four of the six observation-based products that produced annual NEE estimates (figure 2(c)). Previous studies have expressed concern that process-model underestimation of fall and winter high-latitude C fluxes (Commane *et al* 2017, Natali *et al* 2019) has led to an incorrect characterization of the region as a C sink.

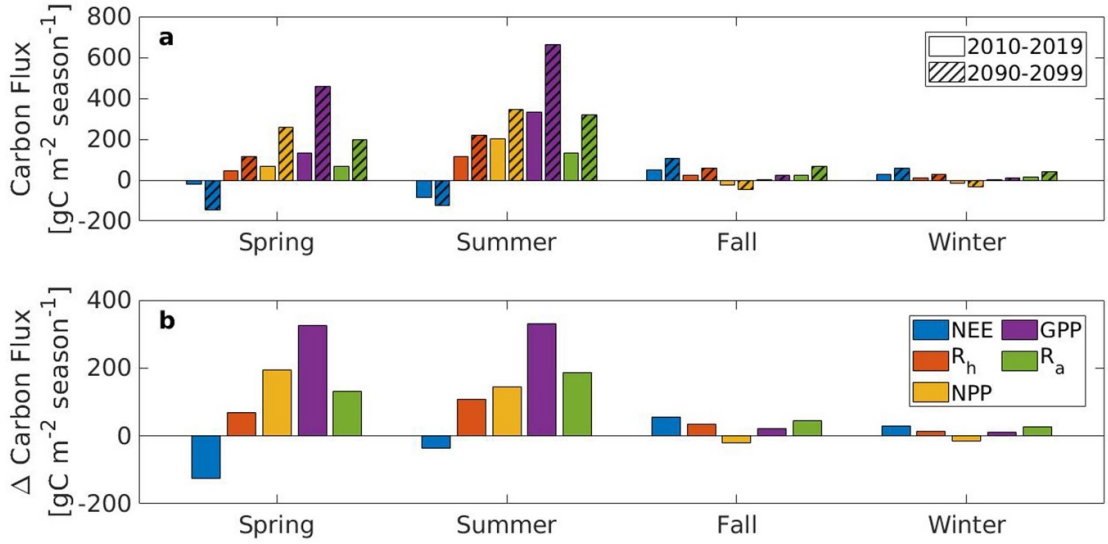

Figure 3. Large relative changes in Alaska spring C fluxes will control annual C budgets by 2100. (a) Seasonal NEE (blue), microbial respiration (denoted as R_h, red), NPP (yellow), GPP (purple), and autotrophic respiration (denoted as R_a, green) averaged across Alaska for the years 2010–2019 (open) and 2090–2099 (hashed). (b) Difference between 2090–2099 and 2010–2019 Alaskan seasonal C fluxes. The seasons are equinox based.

However, ecosys predicted a 27 gC m^{-2} (50%) larger combined fall and winter CO_2 flux than the average of the observation-based products, while still predicting that Alaska is currently a net C sink.

Under current climate conditions, modeled Alaska NEE for years 2000–2019 is largest in magnitude during summer (figure 3). Modeled summer dominance of the Alaskan C cycle is corroborated by the site measurements and 4 of the 6 observation-based products discussed above (figures 2(b) and (d)). The NEE seasonality of the observation-based products is broadly consistent with modeled NEE seasonality (table S3). These comparisons, and those described in the supplementary material, give confidence that *ecosys* is reasonably capturing the C cycle seasonality across our study domain.

3.2. Future changes to the spring C cycle

To assess how C cycle seasonality will change across Alaska with climate warming, we ran *ecosys* through the year 2100 using a CCSM4 RCP8.5 scenario. In spring (21 March–20 June), modeled NPP increases from 66 to 260 gC m^{-2} $season^{-1}$ by year 2100 (positive NPP signifies positive plant growth; figure 3). This large increase in spring C fixation is driven by increases in air temperature (on average 6.7 °C by year 2100, figure S5) that lead to enhanced C fixation rates and earlier C uptake, particularly since temperature sensitivity of fixation rates is larger at lower temperatures (Kirschbaum 1995). Growing season onset (defined as the first day that modeled NPP is positive) in Alaska advances by 39 d by the year 2100 (5.8 d $°C^{-1}$; figure S7), consistent with published estimates of leafout advancement sensitivities in the northern hemisphere (Xu *et al* (2019): −1 to −4.5 d $°C^{-1}$; Piao *et al* (2015): −4.3 d $°C^{-1}$; Linkosalo *et al* (2009): −2.2 to −7.3 d $°C^{-1}$). Current observations of the effect of interannual variation in spring temperatures on high-latitude leaf emergence (Arft *et al* 1999, Pop *et al* 2000, Bjorkman *et al* 2020), growing season length (Chapin *et al* 1996, Keeling *et al* 1996, Myneni *et al* 1997), and plant productivity (Hicke *et al* 2002, Piao *et al* 2007) confirm that high-latitude plants experience severe temperature limitations during spring.

We quantified temperature and radiation limitations to modeled plant productivity using breakpoint regression analysis of daily air temperatures, incoming SW radiation, and modeled NPP (figure S6, Methods, Keenan and Riley 2018). According to this method, NPP is considered to be limited by, e.g. cold temperatures, if outlying NPP values increase at warmer temperatures. Under current Alaska climate conditions, modeled NPP experiences a 61% limitation due to air temperature in the spring. By year 2100, however, spring temperature limitation to NPP will relax by more than a factor of 3 (to 19%; figure S6). Since incoming shortwave radiation during these months is high, photosynthetic activity can respond positively to warmer spring temperatures. The geographically weighted regression coefficient (R^2) between spring temperature limitation and spring NPP remains high (0.83–0.85) throughout the century for the study domain (figure 4), providing confirmation that temperature remains a primary control of spring NPP throughout the century.

Modeled spring microbial respiration (denoted as R_h in figure 3) increases from 48 to 116 gC m^{-2} $season^{-1}$ throughout the century in response to earlier snowmelt and warmer soil temperatures. Soil temperatures increase more slowly than air temperatures in the spring (figure S5), so the increase

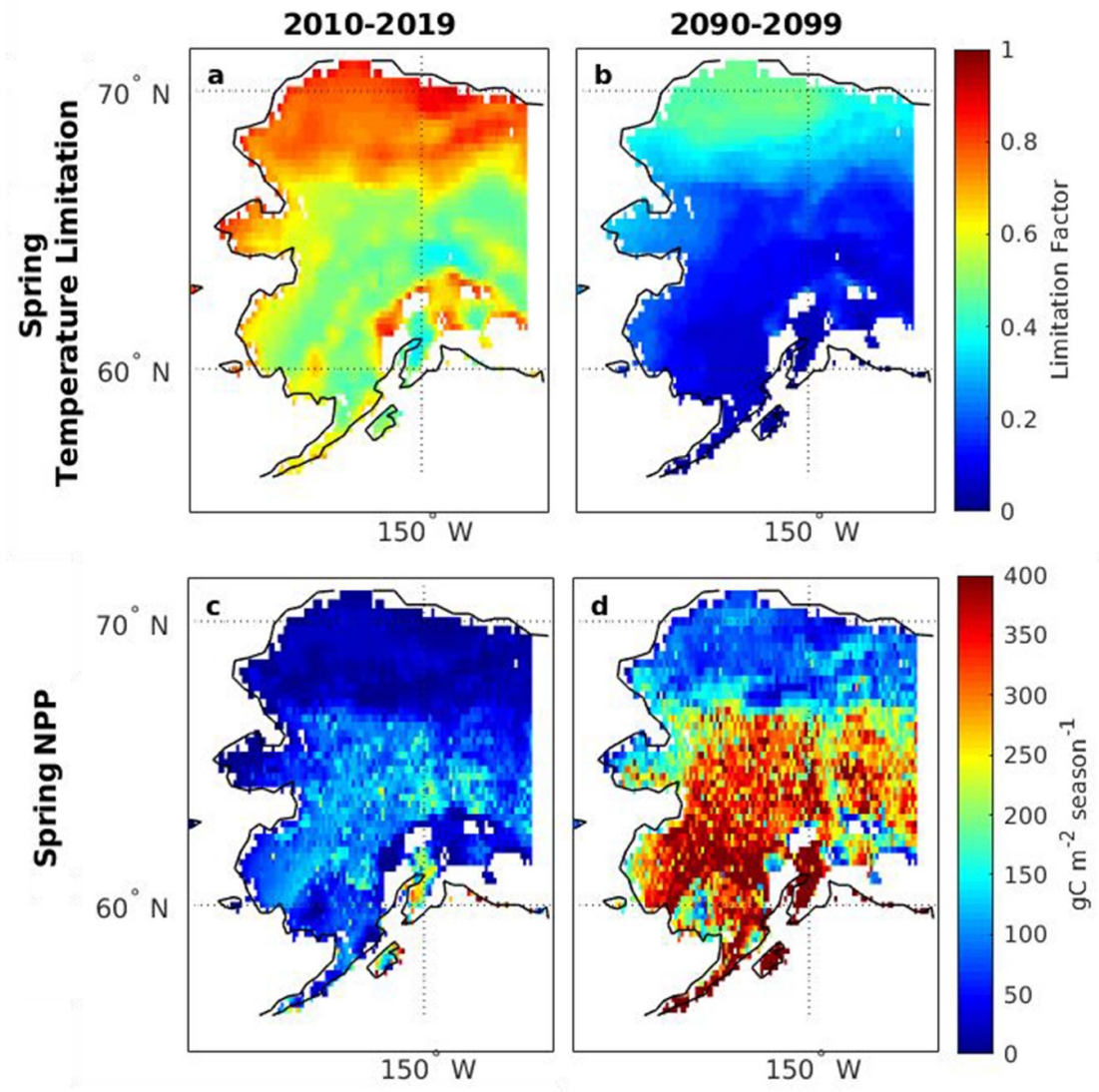

Figure 4. Spatial distribution of spring NPP matches spatial distribution of spring temperature limitation throughout the 21st century. Spring temperature limitation (a), (b) and spring NPP (c), (d) are strongly correlated (geographically weighted regression coefficient (R^2) of 0.83 for the years 2010–2019 (a), (c) and 0.85 for the years 2090–2099 (b), (d)). The seasons are equinox based.

in microbial respiration is much smaller than the projected increase in NPP. This difference results in a very large increase in the magnitude of spring NEE by year 2100 (−19 to −144 g C m^{-2} $season^{-1}$; figure 3(a)).

3.3. Future changes to the summer C cycle

In summer (21 June–20 September), modeled NPP increases from 201 to 344 gC m^{-2} $season^{-1}$ throughout the century (figure 3(a)). Similar increases in spring and summer air temperature (∼6 °C–7 °C; figure S5) lead to similar increases in spring and summer Alaska GPP by year 2100 (326 *vs.* 331 gC m^{-2}; figure 3). However, higher baseline air temperatures during summer lead to larger increases in autotrophic respiration (187 gC m^{-2} in summer vs. 132 gC m^{-2} in spring; denoted as R_a in figure 3), resulting in smaller increases in NPP compared to spring (figures 3 and S5).

Some studies have hypothesized that increases in growing season water stress may lead to a reduction in summer GPP (Buermann *et al* 2013, Liu *et al* 2020). Consistent with these studies, the impact of warming on summer water stress has been demonstrated using *ecosys* in an analysis of boreal forest dynamics (Grant *et al* 2009). In this study, we find that increasing summer water stress is buffered by increasing precipitation and increasing atmospheric CO_2 concentrations that reduce transpiration. The RCP8.5 climate forcing we applied here (Methods) predicts a 22% increase in summer precipitation across Alaska (figure S5), consistent with studies that suggest rainfall is projected to increase with warming at high latitudes (Bintanja and Andry 2017). As a result, we predicted slightly wetter summer soils, almost no change in summer evapotranspiration (0.4% decrease), and a small increase (∼16%) in summer water stress (calculated as the number of hours that the canopy water

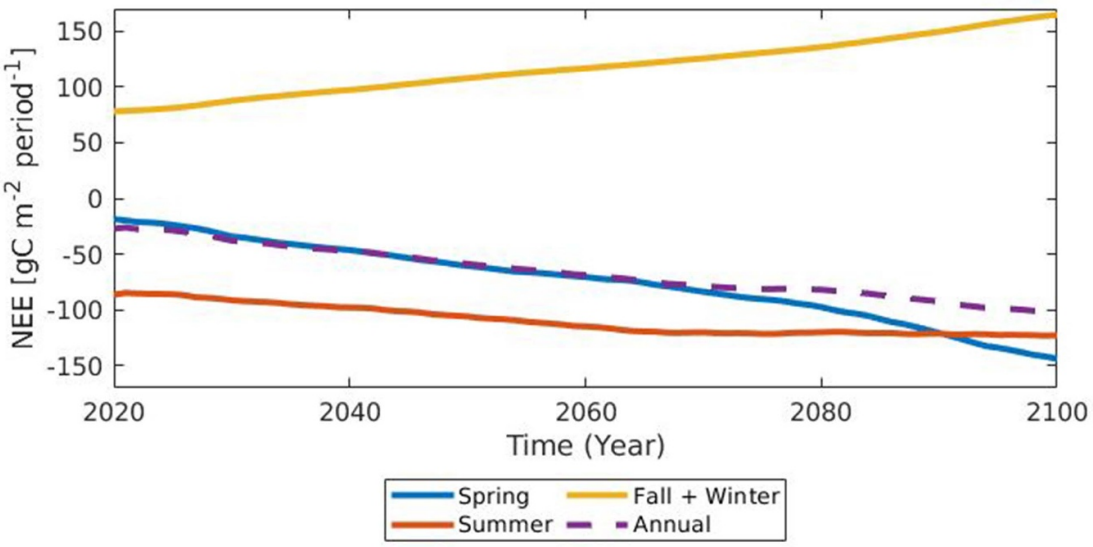

Figure 5. Spring net C uptake becomes larger than summer uptake by year 2100. 10 year rolling mean of Alaska spring (blue), summer (red), combined fall and winter (yellow), and annual (purple) NEE for the years 2020–2100. The seasons are equinox based.

potential drops below a threshold value; Methods) across Alaska by year 2100.

Modeled summer microbial respiration increases from 114 to 221 gC m^{-2} $season^{-1}$ throughout the century (figure 3). This increase is larger than that during spring because there are larger plant litter inputs and warmer and drier soils in summer than in spring. Summer net C uptake is projected to increase by only 36 gC m^{-2}, which is much smaller than the increase in spring net C uptake. By year 2100, summer net C uptake (123 gC m^{-2} $season^{-1}$) is less than spring net C uptake (144 gC m^{-2} $season^{-1}$) across Alaska (figures 3 and 5).

3.4. Future changes to the fall and winter C cycle

In fall (21 September–20 December) and winter (21 December–20 March), there is only a small change in NPP throughout the century (21 gC m^{-2} $season^{-1}$ for fall and 16 gC m^{-2} $season^{-1}$ for winter). In fall, the current complete temperature limitation reduces to a partial limitation by year 2100 (figure S6). However, day lengths during fall in Alaska are very short, and there is not enough sunlight to drive photosynthesis. Since incoming shortwave radiation seasonality is driven primarily by earth-sun geometry (i.e. not climate change), the extreme radiation limitation to fall and winter NPP is not expected to change significantly over the coming century (Holland and Landrum 2015). In fall, temperature and radiation are each currently strongly limiting, but by year 2100 radiation will become the dominant limiting factor to fall C fixation. This prediction is consistent with observed large-scale increases in radiation limitation across northern latitudes (Zhang *et al* 2020).

By year 2100, average fall soil temperatures increase from −1.3 °C to 0.8 °C, average winter soil temperatures increase from −3.0 °C to −0.9 °C, and the first frost (defined as the date when surface soil temperature first drops below −0.2 °C) is delayed by one month on average. Modeled microbial respiration by year 2100 increases in response to warming soil temperatures from 25 to 61 gC m^{-2} $season^{-1}$ in fall, and from 15 to 31 gC m^{-2} $season^{-1}$ in winter. Net C loss during fall and winter is projected to shift from 76 gC m^{-2} $season^{-1}$ (88% of summer net C uptake) to 163 gC m^{-2} $season^{-1}$ (133% of summer net C uptake) over the course of the century (figures 3 and 5). Adding in the large increase in spring net C uptake, modeled annual Alaska NEE will increase in magnitude from −30 gC m^{-2} y^{-1} in the current decade to −108 gC m^{-2} y^{-1} by year 2100 (figure 5).

3.5. Fall and winter N cycle is linked to spring C cycle

Whereas most large-scale land models link plant nutrient acquisition with instantaneous photosynthetic demand, *ecosys* allows plants to use non-structural C reserves to uptake and store nutrients whenever they are available (Riley *et al* 2018, 2021). In the model, rates of mineralization and N fixation (symbiotic and non-symbiotic) control soil N availability and depend on soil temperature and liquid water availability. During fall and winter, modeled plant N uptake varies with the number of days that soil temperatures at 5 cm depth remain above freezing ($R^2 = 0.60$). Throughout the 21st century, the number of days above freezing increases from 21 to 60 d, synchronous with an increase in fall and winter plant N uptake from 0.26 to 0.69 gN m^{-2} (figure 6(a)).

Nutrient acquisition during the fall and winter has been shown to strongly influence year-round vegetation growth and competitive dynamics in

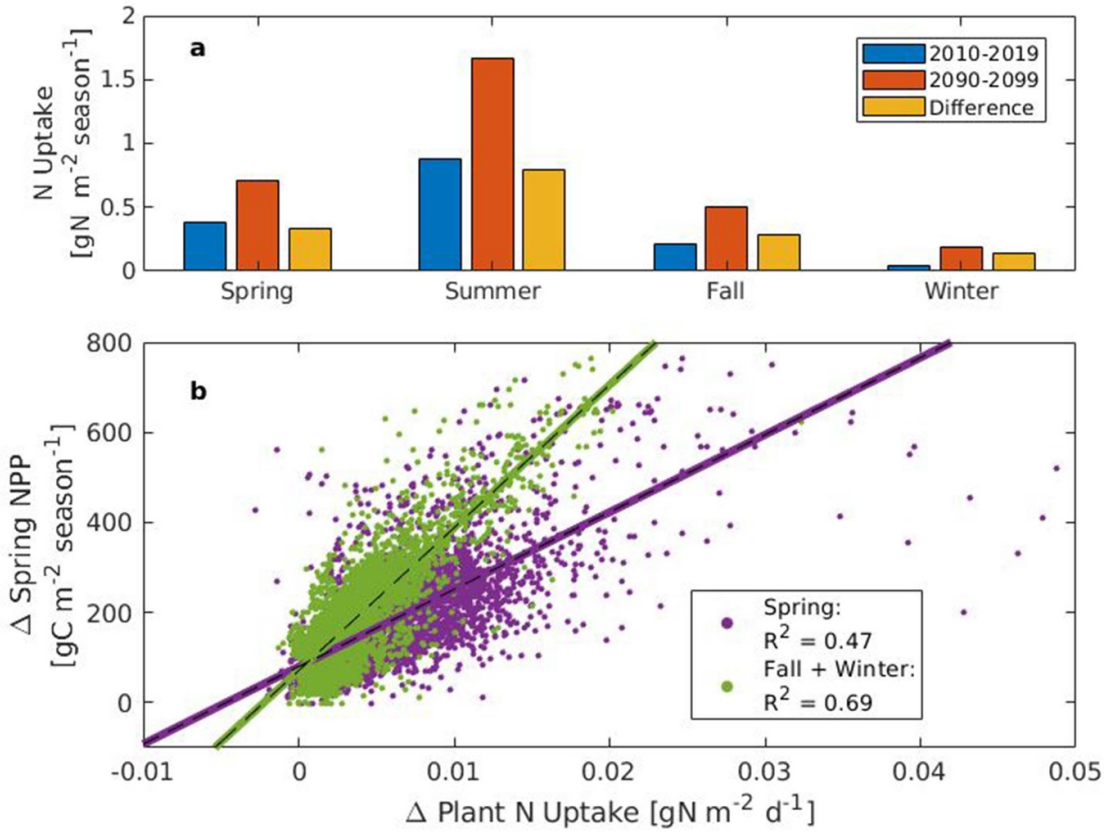

Figure 6. Increasing fall and winter plant N uptake drives increasing spring NPP. (a) Seasonal plant N uptake in each grid cell is shown for the years 2010–2019 (blue) and 2090–2099 (red). The difference between the two decades for each variable is shown in yellow. (b) Differences in spring NPP between 2090–2099 and 2010–2019 are plotted against differences in mean daily plant N uptake during spring (purple) and fall and winter (green) for the same period. The seasons are equinox based.

northern ecosystems (Chapin and Bloom 1976, Larsen *et al* 2012, Malyshev and Henry 2012). By the end of the century, 22.5% of modeled plant N acquisition occurs during fall and winter, and it is likely that the large increase in spring productivity discussed above would not be possible without this source of N. Indeed, we find that modeled increases in spring NPP throughout the century are more strongly correlated with increases in fall and winter plant N uptake ($R^2 = 0.69$) than with increases in spring plant N uptake ($R^2 = 0.47$; figure 6). This result highlights the importance of accounting for fall and winter plant nutrient uptake in predictions of seasonal and annual high-latitude ecosystem response to climate change.

3.6. Caveats and uncertainties

Some processes important to ecosystem C balance and export, such as topography, landscape-scale hydrology, thermokarst, and other geomorphological dynamics, are not represented in these model runs. Additionally, since boreal forest PFT species are not initialized in regions of present-day tundra, boreal treeline advance, which has been observed across the high-latitudes (Harsch *et al* 2009), does not occur in these simulations. However, trends in the seasonality of terrestrial ecosystem C exchange identified here are expected to be robust since they are attributed primarily to seasonal light availability driven by earth-sun geometry and large-scale shifts in seasonal temperature driven by climate change. As is the case for all model analyses of ecosystem dynamics, there is uncertainty associated with the gridded climate data and soil information we used to force *ecosys* (Mekonnen *et al* 2016, Wang and Clow 2021). Biases in temperature forcing data would affect the rates of processes (e.g. maximum fixation rates, electron transport rates) that drive modeled plant productivity and microbial respiration. While this uncertainty has an impact on comparisons between *ecosys* and observation-based products, it does not affect our conclusions, as we show using a sensitivity analysis (supplementary material).

4. Conclusions

We show that 21st century climate warming will shift C cycle seasonality across Alaska. Spring C sink strength will become larger than summer C sink strength by year 2100 due to relaxation of temperature limitations to plant productivity and nutrient availability. This result represents a striking, and to our knowledge, previously unreported shift in the timing of high-latitude net C uptake. Severe radiation

limitation to NPP in fall and winter is not projected to change, so increased temperatures during these months will not benefit plant C uptake. Instead, warming soils and increased plant inputs will lead to higher rates of autotrophic and microbial respiration, and net C loss during the fall and winter will become larger than net C uptake during the summer by year 2100. Further investigation is needed to ascertain the impacts of shifting C cycle seasonality, and associated changes in energy and water fluxes, on climate.

Our results address the conflict between modeled and observation-based assessments of high-latitude ecosystem C balance. Our model predictions of large and increasing fall and winter C losses are consistent with observation-based estimates produced by Natali *et al* (2019) and Commane *et al* (2017), unlike most process models referenced in those studies. However, our results also agree with the process model consensus that high-latitudes will remain a C sink throughout the 21st century. This result is attributable in part to increased N mineralization and plant nutrient uptake coincident with fall and winter C losses. Nevertheless, data used to build observation-based products and to parameterize and validate process models is very sparse at high-latitudes. Increased spatial and temporal coverage of measured ecosystem C fluxes would be very helpful to verify the trends predicted here, and to further close the gap between mechanistically modeled and observation-based estimates of seasonal C fluxes.

Data availability statement

The data that support the findings of this study are openly available at the following URL/DOI: https://ngee-arctic.ornl.gov/. Data will be available from 22 December 2021.

Acknowledgments

This research was supported by the U.S. Department of Energy, Office of Science, Office of Biological and Environmental Research under Contract No. DE-AC02-05CH11231 to Lawrence Berkeley National Laboratory as part of the Next-Generation Ecosystem Experiments in the Arctic (NGEE-Arctic) project.

ORCID iDs

Ian A Shirley https://orcid.org/0000-0002-2229-1414
Zelalem A Mekonnen https://orcid.org/0000-0002-2647-0671
Baptiste Dafflon https://orcid.org/0000-0001-9871-5650
William J Riley https://orcid.org/0000-0002-4615-2304

References

Arft A M *et al* 1999 Responses of tundra plants to experimental warming: meta-analysis of the international tundra experiment *Ecol. Monogr.* **69** 491–511
Arora V K and Boer G J 2014 Terrestrial ecosystems response to future changes in climate and atmospheric CO_2 concentration *Biogeosciences* **11** 4157–71
Billings W D 1973 Arctic and alpine vegetations: similarities, differences, and susceptibility to disturbance *BioScience* **23** 697–704
Bintanja R and Andry O 2017 Towards a rain-dominated Arctic *Nat. Clim. Change* **7** 263–7
Bjorkman A D *et al* 2020 Status and trends in Arctic vegetation: evidence from experimental warming and long-term monitoring *Ambio* **49** 678–92
Bouskill N J, Riley W J, Zhu Q, Mekonnen Z A and Grant R F 2020 Alaskan carbon-climate feedbacks will be weaker than inferred from short-term experiments *Nat. Commun.* **11** 1–12
Box J E *et al* 2019 Key indicators of Arctic climate change: 1971–2017 *Environ. Res. Lett.* **14** 045010
Buermann W, Bikash P R, Jung M, Burn D H and Reichstein M 2013 Earlier springs decrease peak summer productivity in North American boreal forests *Environ. Res. Lett.* **8** 024027
Chapin F S and Bloom A 1976 Phosphate absorption: adaptation of tundra graminoids to a low temperature, low phosphorus environment *Oikos* **27** 111
Chapin F S, Bret-Harte M S, Hobbie S E and Zhong H 1996 Plant functional types as predictors of transient responses of arctic vegetation to global change *J. Veg. Sci.* **7** 347–58
Commane R *et al* 2017 Carbon dioxide sources from Alaska driven by increasing early winter respiration from Arctic tundra *Proc. Natl Acad. Sci. USA* **114** 5361–6
Dentener F J 2006 Global maps of atmospheric nitrogen deposition, 1860, 1993, and 2050 *ORNL Distributed Active Archive Center Datasets* (https://doi.org/10.3334/ornldaac/830)
Donohue R J, Roderick M L, McVicar T R and Farquhar G D 2013 Impact of CO_2 fertilization on maximum foliage cover across the globe's warm, arid environments *Geophys. Res. Lett.* **40** 3031–5
Ernakovich J G, Hopping K A, Berdanier A B, Simpson R T, Kachergis E J, Steltzer H and Wallenstein M D 2014 Predicted responses of arctic and alpine ecosystems to altered seasonality under climate change *Glob. Change Biol.* **20** 3256–69
Farquhar G D, Von Caemmerer S and Berry J A 1980 A biochemical model of photosynthetic CO_2 assimilation in leaves of C3 species *Planta* **149** 78–90
Gallego-Sala A V *et al* 2018 Latitudinal limits to the predicted increase of the peatland carbon sink with warming *Nat. Clim. Change* **8** 907–13
Grant R F 2014 Nitrogen mineralization drives the response of forest productivity to soil warming: modelling in ecosys vs. measurements from the Harvard soil heating experiment *Ecol. Model.* **288** 38–46
Grant R F and Baldocchi D D 1992 Energy transfer over crop canopies: simulation and experimental verification *Agric. For. Meteorol.* **61** 129–49
Grant R F, Barr A G, Black T A, Margolis H A, Dunn A L, Metsaranta J, Wang S, McCaughey J H and Bourque C A 2009 Interannual variation in net ecosystem productivity of Canadian forests as affected by regional weather patterns—a Fluxnet-Canada synthesis *Agric. For. Meteorol.* **149** 2022–39
Grant R F and Flanagan L B 2007 Modeling stomatal and nonstomatal effects of water deficits on CO_2 fixation in a semiarid grassland *J. Geophys. Res. Biogeosci.* **112** G03011
Grant R F, Humphreys E R and Lafleur P M 2015 Ecosystem CO_2 and CH_4 exchange in a mixed tundra and a fen within a hydrologically diverse Arctic landscape: 1. Modeling versus measurements *J. Geophys. Res. Biogeosci.* **120** 1366–87

Grant R F, Humphreys E R, Lafleur P M and Dimitrov D D 2011 Ecological controls on net ecosystem productivity of a mesic arctic tundra under current and future climates *J. Geophys. Res.* **116** G01031

Grant R F, Jarvis P G, Massheder J M, Hale S E, Moncrieff J B, Rayment M, Scott S L and Berry J A 2001 Controls on carbon and energy exchange by a black spruce-moss ecosystem: testing the mathematical model *Ecosys* with data from the BOREAS experiment *Glob. Biogeochem. Cycles* **15** 129–47

Grant R F, Mekonnen Z A, Riley W J, Arora B and Torn M S 2017 Mathematical modelling of Arctic polygonal tundra with ecosys: 2. microtopography determines how CO_2 and CH_4 exchange responds to changes in temperature and precipitation *J. Geophys. Res. Biogeosci.* **122** 3174–87

Grant R 2001 A review of the Canadian ecosystem model—ecosys *Modeling Carbon and Nitrogen Dynamics for Soil Management* (Boca Raton, FL: Lewis Publishers) p 91

Graven H D *et al* 2013 Enhanced seasonal exchange of CO2 by northern ecosystems since 1960 *Science* **341** 1085–9

Harsch M A, Hulme P E, McGlone M S and Duncan R P 2009 Are treelines advancing? A global meta-analysis of treeline response to climate warming *Ecol. Lett.* **12** 1040–9

Hicke J A, Asner G P, Randerson J T, Tucker C, Los S, Birdsey R, Jenkins J C, Field C and Holland E 2002 Satellite-derived increases in net primary productivity across North America, 1982–1998 *Geophys. Res. Lett.* **29** 69-1–4

Holland M M and Landrum L 2015 Factors affecting projected Arctic surface shortwave heating and albedo change in coupled climate models *Phil. Trans. R. Soc.* A **373** 20140162

Hugelius G *et al* 2013 Short communication: a new dataset for estimating organic carbon storage to 3 m depth in soils of the northern circumpolar permafrost region *Earth Syst. Sci. Data Discuss.* **5** 393–402

Ito A, Nishina K and Noda H M 2016 Impacts of future climate change on the carbon budget of northern high-latitude terrestrial ecosystems: an analysis using ISI-MIP data *Polar Sci.* **10** 346–55

Jacobson A R *et al* 2020 CarbonTracker CT2019 (https://doi.org/10.25925/39M3-6069)

Jung M *et al* 2020 Scaling carbon fluxes from eddy covariance sites to globe: synthesis and evaluation of the FLUXCOM approach *Biogeosciences* **17** 1343–65

Keeling C D, Chin J F S and Whorf T P 1996 Increased activity of northern vegetation inferred from atmospheric CO_2 measurements *Nature* **382** 146–9

Keenan T F and Riley W J 2018 Greening of the land surface in the world's cold regions consistent with recent warming *Nat. Clim. Change* **8** 825–8

Kirschbaum M U F 1995 The temperature dependence of soil organic matter decomposition, and the effect of global warming on soil organic C storage *Soil Biol. Biochem.* **27** 753–60

Larsen K S, Michelsen A, Jonasson S, Beier C and Grogan P 2012 Nitrogen uptake during fall, winter and spring differs among plant functional groups in a subarctic heath ecosystem *Ecosystems* **15** 927–39

Lawrence D M, Koven C D, Swenson S C, Riley W J and Slater A G 2015 Permafrost thaw and resulting soil moisture changes regulate projected high-latitude CO_2 and CH_4 emissions *Environ. Res. Lett.* **10** 094011

Lee H, Swenson S C, Slater A G and Lawrence D M 2014 Effects of excess ground ice on projections of permafrost in a warming climate *Environ. Res. Lett.* **9** 124006

Leffler A J, Klein E S, Oberbauer S F and Welker J M 2016 Coupled long-term summer warming and deeper snow alters species composition and stimulates gross primary productivity in tussock tundra *Oecologia* **181** 287–97

Linkosalo T, Häkkinen R, Terhivuo J, Tuomenvirta H and Hari P 2009 The time series of flowering and leaf bud burst of boreal trees (1846–2005) support the direct temperature observations of climatic warming *Agric. For. Meteorol.* **149** 453–61

Liu S, Wei Y, Post W M, Cook R B, Schaefer K and Thornton M M 2013 The unified North American soil map and its implication on the soil organic carbon stock in North America *Biogeosciences* **10** 2915–30

Liu Z *et al* 2020 Increased high-latitude photosynthetic carbon gain offset by respiration carbon loss during an anomalous warm winter to spring transition *Glob. Change Biol.* **26** 682–96

Malyshev A V and Henry H A L 2012 Frost damage and winter nitrogen uptake by the grass Poa pratensis L.: consequences for vegetative versus reproductive growth *Plant Ecol.* **213** 1739–47

McGuire A D *et al* 2012 An assessment of the carbon balance of Arctic tundra: comparisons among observations, process models, and atmospheric inversions *Biogeosciences* **9** 3185–204

McGuire A D *et al* 2018 Dependence of the evolution of carbon dynamics in the northern permafrost region on the trajectory of climate change *Proc. Natl Acad. Sci. USA* **115** 3882–7

Mekonnen Z A, Grant R F and Schwalm C 2016 Sensitivity of modeled NEP to climate forcing and soil at site and regional scales: implications for upscaling ecosystem models *Ecol. Model.* **320** 241–57

Mekonnen Z A, Riley W J and Grant R F 2018 21st century tundra shrubification could enhance net carbon uptake of North America Arctic tundra under an RCP8.5 climate trajectory *Environ. Res. Lett.* **13** 054029

Mekonnen Z A, Riley W J, Grant R F and Romanovsky V E 2021 Changes in precipitation and air temperature contribute comparably to permafrost degradation in a warmer climate *Environ. Res. Lett.* **16** 024008

Mekonnen Z A, Riley W J, Randerson J T, Grant R F and Rogers B M 2019 Expansion of high-latitude deciduous forests driven by interactions between climate warming and fire *Nat. Plants* **5** 952–8

Mikan C J, Schimel J P and Doyle A P 2002 Temperature controls of microbial respiration in arctic tundra soils above and below freezing *Soil Biol. Biochem.* **34** 1785–95

Myneni R B, Keeling C D, Tucker C J, Asrar G and Nemani R R 1997 Increased plant growth in the northern high latitudes from 1981 to 1991 *Nature* **386** 698–702

Natali S M *et al* 2019 Large loss of CO 2 in winter observed across the northern permafrost region *Nat. Clim. Change* **9** 852–7

Parazoo N C, Koven C D, Lawrence D M, Romanovsky V and Miller C E 2018 Detecting the permafrost carbon feedback: talik formation and increased cold-season respiration as precursors to sink-to-source transitions *Cryosphere* **12** 123–44

Piao S *et al* 2015 Leaf onset in the northern hemisphere triggered by daytime temperature *Nat. Commun.* **6** 6911

Piao S, Friedlingstein P, Ciais P, Viovy N and Demarty J 2007 Growing season extension and its impact on terrestrial carbon cycle in the Northern Hemisphere over the past 2 decades *Glob. Biogeochem. Cycles* **21** GB3018

Pop E W, Oberbauer S F and Starr G 2000 Predicting vegetative bud break in two arctic deciduous shrub species, Salix pulchra and Betula nana *Oecologia* **124** 176–84

Riley W J, Mekonnen Z A, Tang J, Zhu Q, Bouskill N J and Grant R F 2021 Non-growing season plant nutrient uptake controls Arctic tundra vegetation composition under future climate *Environ. Res. Lett.* **16** 074047

Riley W J, Zhu Q and Tang J Y 2018 Weaker land–climate feedbacks from nutrient uptake during photosynthesis-inactive periods *Nat. Clim. Change* **8** 1002–6

Rogelj J, Forster P M, Kriegler E, Smith C J and Séférian R 2019 Estimating and tracking the remaining carbon budget for stringent climate targets *Nature* **571** 335–42

Rollins M G 2009 LANDFIRE: a nationally consistent vegetation, wildland fire, and fuel assessment *Int. J. Wildland Fire* **18** 235

Schaefer G L, Cosh M H and Jackson T J 2007 The USDA natural resources conservation service soil climate analysis network (SCAN) *J. Atmos. Ocean. Technol.* **24** 2073–7

Schuur E A G *et al* 2015 Climate change and the permafrost carbon feedback *Nature* **520** 171–9

Serreze M C, Barrett A P, Stroeve J C, Kindig D N and Holland M M 2009 The emergence of surface-based Arctic amplification *Cryosphere* **3** 11–19

Serreze M C and Barry R G 2011 Processes and impacts of Arctic amplification: a research synthesis *Glob. Planet. Change* **77** 85–96

Tharammal T, Bala G, Devaraju N and Nemani R 2019 A review of the major drivers of the terrestrial carbon uptake: model-based assessments, consensus, and uncertainties *Environ. Res. Lett.* **14** 093005

Ukkola A M, Colin Prentice I, Keenan T F, van Dijk A I, Viney N R, Myneni R B and Bi J 2016 Reduced streamflow in water-stressed climates consistent with CO_2 effects on vegetation *Nat. Clim. Change* **6** 75–78

USDA Natural Resources Conservation Service 2020 Snowpack telemetry network (SNOTEL)

Wang K and Clow G D 2021 Newly collected data across Alaska reveal remarkable biases in solar radiation products *Int. J. Climatol.* **41** 497–512

Wei Y *et al* 2014 The North American carbon program multi-scale synthesis and terrestrial model intercomparison project—part 2: environmental driver data *Geosci. Model Dev.* **7** 2875–93

Wieder W R, Cleveland C C, Lawrence D M and Bonan G B 2015 Effects of model structural uncertainty on carbon cycle projections: biological nitrogen fixation as a case study *Environ. Res. Lett.* **10** 044016

Winkler A J, Myneni R B, Alexandrov G A and Brovkin V 2019 Earth system models underestimate carbon fixation by plants in the high latitudes *Nat. Commun.* **10** 885

Xu X, Riley W J, Koven C D and Jia G 2018 Observed and simulated sensitivities of spring greenup to preseason climate in Northern Temperate and Boreal Regions *J. Geophys. Res. Biogeosci.* **123** 60–78

Xu X, Riley W J, Koven C D and Jia G 2019 Heterogeneous spring phenology shifts affected by climate: supportive evidence from two remotely sensed vegetation indices *Environ. Res. Commun.* **1** 091004

Zeng J, Matsunaga T, Tan Z-H, Saigusa N, Shirai T, Tang Y, Peng S and Fukuda Y 2020 Global terrestrial carbon fluxes of 1999–2019 estimated by upscaling eddy covariance data with a random forest *Sci. Data* **7** 313

Zhang Y, Commane R, Zhou S, Park Williams A and Gentine P 2020 Light limitation regulates the response of autumn terrestrial carbon uptake to warming *Nat. Clim. Change* **10** 739–43